Desalination and Water Treatment
www.deswater.com

doi: 10.5004/dwt.2023.29798

303 (2023) 212–223
August

Adsorption of Rhodamine B dye on potassium permanganate modified peanut shell: adsorption kinetics, thermodynamics and isotherm studies

Qing-Zhou Zhai

Research Center for Nanotechnology, South Campus, Changchun University of Science and Technology, 7186 Weixing Road, Changchun 130022, China, email: zhaiqingzhou@163.com

Received 3 May 2023; Accepted 20 July 2023

ABSTRACT

In order to study the adsorption effect of peanut shell on dye in industrial wastewater, the dye Rhodamine B was used as the research object and the peanut shell was modified. After modification, the best adsorption effect is potassium permanganate modified materials. The factors affecting the adsorption of Rhodamine B on peanut shell, such as pH value, initial concentration of dye, amount of adsorbent, contact time, adsorption temperature and ionic strength, were investigated. The best adsorption conditions of peanut shell for Rhodamine B were obtained. The adsorption thermodynamic equation, adsorption kinetic equation and the sorption isotherms were determined. The results showed that the adsorption process satisfied Freundlich isothermal adsorption equation and the adsorption process was spontaneous and exothermic. The adsorption of Rhodamine B on peanut shell accorded with the pseudo-second-order adsorption kinetics.

Keywords: Rhodamine B; Modified peanut shell; Adsorption; Kinetics; Thermodynamics; Isotherm

1. Introduction

Dye has toxicity and affects the animals in the water. Perhaps it may lead to mutations or deformities in the water organisms, or even cancer. Human kidney function may therefore be thus disrupted, reproductive and liver functions are thus affected, and dye pollution can still damage the brain and nervous system [1–3]. Rhodamine B (RB, $C_{27}H_{34}N_2O_4S$) is an alkaline dye (Table 1). Its wastewater has deep color, large biotoxicity, difficult biodegradation. The dye is highly resistant to photohydrolysis and the anti-oxidation is strong. Rhodamine B is a well-known water tracer fluorescent and has been widely used as a colorant in textiles and food stuffs. It is harmful to the respiratory tract, skin and eyes. It also has the carcinogenicity, reproductive and developmental toxicity, neurotoxicity and chronic toxicity towards humans and animals [4,5]. Dye wastewater is usually treated with physical, chemical treatment, or bioremediation techniques. These include physicochemical methods, membrane filtration, electrocoagulation, electrochemical destruction, ion exchange, irradiation, precipitation, and smelly oxidation. However, these techniques are generally ineffective for color removal, costly, or produce disadvantages such as secondary pollution, and are barely adaptable to a wide range of dye wastewater. Adsorption is the most effective in advanced wastewater treatment, and industry uses adsorption to reduce the harmful pollutants existing in the wastewater. Adsorption is an efficient, renewable, and environmentally friendly method [6–10]. Adsorption is an effective way found to remove color from dye wastewater. At the present stage, adsorption method is mainly applied to the treatment of wastewater containing heavy metal ions, dyes, phosphorus, phenol, antibiotics, but because commercial adsorbent cannot well adapt to the huge market, the problem of developing new, highly efficient and high-quality adsorbent is urgent to be solved [11–17]. Methylene blue [18], crystal violet [19–22], titan yellow [23], tropaeoline 000 [24], chrysoidine R [25], eosin Y [26],

Cd^{2+} [27,28], Cr(VI) [28], Pb^{2+}, Cu^{2+}, Ni^{2+} [29] have been studied by adsorption method. Activated carbon adsorption is an effective decolor method, but high price, desorption regeneration is difficult, difficult to promote and use. Many studies have been carried out to find low-cost absorbers including peat, bentonite, steel mill slag, ashes, porcelain soil, corn cobs, plannings and silica [2]. Lignin cellulose biomass is an effective adsorbent that acts as good. Using different physical or chemical treatments can improve the adsorption capacity of these biomass adsorbents. The focus of the current research is the need to replace commercial activated carbon as a cost-effective but potential adsorbent. Many researchers have reported the feasibility of using a variety of low-cost adsorbent from natural materials, industrial solid waste, agricultural by-products and biological adsorbent as a precursor [2,14].

China is the world's largest producer of peanut. Peanut shells are abundant but low utilization and are only commonly used as animal feed. Peanut shell is a common agricultural and forestry solid waste. Peanuts contain cellulose, lignin and semifiber up to 44.15%, 32.60% and 3.76%, with adsorption performance. Also, through appropriate surface chemical modification, its adsorption performance is improved. Peanut shell has the advantages of rich resources, cheap price and excellent adsorption performance. Peanut shell has high porosity, large surface area, more adsorption function group, and is an efficient adsorbent. Using peanut shell as an adsorbent has gradually become the hot topic of heavy metal pollution treatment [3,6]. Certain synthesis of new materials used to remove Rhodamine B requires some cost [2,13].

RB was used as a model in this paper and modified with potassium permanganate as an adsorbent to carry out adsorption study. The influence of various experimental conditions on dye adsorption in water was investigated, and the thermodynamics, dynamics and isotherms of adsorption of RB were investigated, so that the peanut shell can be applied to dye treatment in industrial wastewater. No reports on potassium permanganate modified peanut shell material used for RB adsorption are seen.

2. Experimental set-up

2.1. Reagent and material

Adsorbate: RB ($C_{27}H_{34}N_2O_4S$), was purchased from Suzhou Qihang Biotechnology Science and Technology Co., Ltd., China. Adsorbent: peanut shell was sold by market and purchased from shopping mall in Changchun University of Science and Technology, China. Potassium permanganate, was purchased from Jinan Huijing Chuanshang Trading Co., Ltd., China. All reagents of phosphoric acid, boric acid, acetic acid, sodium hydroxide, hydrochloric acid, sodium chloride and calcium chloride were purchased from Beijing Chemical Plant, China. pH = 4.0 tri-acid (phosphoric acid + boric acid + acetic acid)-sodium hydroxide buffer: 24.5 mL 0.20 mol/L sodium hydroxide solution was added to 100 mL tri-acid (phosphoric acid, acetic acid, boric acid concentration was 0.04 mol/L). The reagent purity was analytical purity. The experimental water was deionized water. The experimental results were an average of 3 parallel measurements.

2.2. Characterization technique

The RB content was determined by spectrophotometry on a 722S spectrophotometer (Shanghai Lengguang Technology Co., Ltd., China). The spectral diagram of the X-ray diffraction (XRD) of sample was determined on a D5005 XRD instrument to obtain crystal phase structure and periodic arrangement characteristics of the sample. Cu-Kα target, $\lambda = 1.5418$ A, operating voltage (tube voltage) 30 kV, operating current (tube current) 20 mA was used with a scanning range of 10°~80°, a step length of 0.2°. Scanning electron microscopy (SEM) photos were measured using Dutch Philips XL30 type field emission scanning electron microscope to observe the particle size and morphology of the sample with an operating voltage of 20 kV. The sample was prepared by ethanol. The sample dropped on the slide for conductive layer treatment. Infrared spectroscopy was recorded on a Nicolet 5DX-FTIR spectrometer (Mike Company, USA) with KBr tablet and a measured range of 400–4,000 cm^{-1}.

2.3. Experimental method

2.3.1. Determination of working curve for RB

In 25 mL measuring flask, 1, 2, 4, 6, 8 and 10 μg/mL RB solution was prepared respectively. At the maximum absorption wavelength of 538 nm, the absorbance of different contents of the RB solution was determined using water as blank and the working curve for the determination of RB was drawn with these data.

2.3.2. Modification of peanut shell

0.2 g peanut shell was boiled with 100 mL water for decoloration 3 times. After the decolourization was complete,

Table 1
Rhodamine B dye information

Dye name	Rhodamine B
Dye index number	81-88-9
Empirical molecular formula	$C_{28}H_{31}ClN_2O_3$
Molecular weight	479.01
Dye content	99%
λ_{max} (nm, experimentally measured)	538 nm
Melting point	210°C–211°C
Solubility	89 mg/mL
Density	0.79 g/cm^3
Supplier	Shanghai Reagent Factory No. 3 (Shanghai, China)
Chemical structure	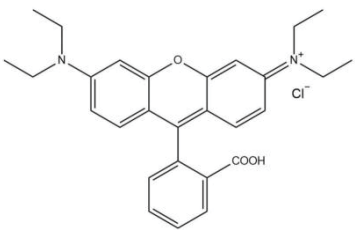

1 g peanut shell was weighed and added to an autoclave. 40 mL 10% (V/V) hydrochloric acid, 10% (W/V) citric acid, 10% (W/V) sodium hydroxide, 10% (W/V) zinc chloride, 10% (W/V) potassium permanganate, 10% (V/V) phosphoric acid was added and then placed to a blast loft drier. The reactant was activated at 120°C for 6 h. It was taken out and after the reactor was completely cooled to room temperature the reactant was filtered. 100 mL water was used to wash 3 times. After the product was stovinged at 60°C for 2 h, it was ground and went through 60 mesh (300 nm) standard sieve and placed in a dryer for standby.

2.3.3. Preparation of potassium permanganate-activated peanut shell

1.0 g of dry peanut shell was added to an autoclave and 40 mL solution of 10% (W/W) $KMnO_4$ was placed in the reactor. The oven temperature was adjusted to 120°C. After reaching the setting value, the reactor was put in the oven and the reactant was activated 120°C for 6 h. After the reactor was taken at rest, the temperature dropped to room temperature and the reactor was opened. The $KMnO_4$ activated peanut shell was taken out and water was added for sucking filtration. 100 mL water was used to wash 3 times until the solution became colorless. The activated peanut shell was put into a blast loft drier, the temperature was adjusted to be 60°C and the product was dried for 2 h. The dried modified peanut shell was ground in a mortar and sifted by a 60 mesh (300 nm) screen mesh, and the powder was placed in a dryer for standby.

2.3.4. Optimum condition for adsorption RB by peanut shell

Effect of the conditional experiment: 10 mL RB solution of 10 μg/mL (Values in parenthesis are experiment of condition, 6–40 μg/mL, the same as below) was added, and respectively placed in 100 mL conical flask. Tri-acid (H_3PO_4-HAc-H_3BO_3)-NaOH buffer solution was respectively used to adjust pH = 4.0 (0–6, pH = 0 system was controlled and regulated by 1 mol/L hydrochloric acid solution medium) and the system was maintained to be 20 mL. 0.2 g (0.1–1.0 g) unmodified peanut shell and $KMnO_4$ modified peanut shell was added. The mixture was stirred for 110 min (unmodified material, the same below) (20–130 min) and 100 min (modified material, the same below) (20–130 min) at room temperature (25°C ± 1°C) (25°C–55°C). The resulting sample was poured into a centrifugal tube. After it was separated for 10 min at 6,000 rpm by centrifugation and the centrifugal tube was taken out, the concentration of RB in the supernatant was determined according to the determination method for above-mentioned RB working curve, and the adsorption ratio and capacity were calculated, so as to obtain the best parameter value of adsorption.

2.3.4.1. Effect of ion strength on adsorption

Eight portions of the RB standard solution of 10 μg/mL was taken, and they were respectively added to 100 mL conical flask. 10 mL pH = 4.0 tri-acid (H_3PO_4-HAc-H_3BO_3)-NaOH buffer solution was used to adjust the acidity of solution. Calcium chloride or sodium chloride were added to the solution with a final concentration of 1 and 0.1 mol/L, respectively. The following experimental operation is the same as the "conditional experimental influence". The effect of the ion strength on the adsorption effect was obtained by comparison.

The relevant calculation formula is as follows:

$$\text{Adsorption ratio } R = \frac{C_0 - C_e}{C_0} \times 100\% \quad (1)$$

$$\text{Equilibrium adsorption capacity } q_e = \left(C_0 - C_e\right) \times \frac{V}{W} \quad (2)$$

where R is adsorption ratio (%), C_0 and C_e are initial concentration and upper supernatant concentration of RB at equilibrium (μg/mL), q_e is equilibrium adsorption capacity (μg/g), V is volume of reaction system (mL), and W is adsorbent weight (g).

2.3.5. Desorption study

0.2 g unmodified waste peanut shell and $KMnO_4$ modified peanut shell were respectively weighed and respectively placed to 100 mL conical flask. 10 mL RB solution of 10 μg/mL was added to each conical flask and 10 mL pH = 4.0 tri-acid-NaOH buffer solution was added, respectively. After the mixture was stirred for 110, 100 min at room temperature by magnetic force, respectively, the resulting sample was added into a centrifugal tube. It was separated for 10 min at 6,000 rpm by centrifugation, the sample for the study of desorption was prepared. 20 mL 0.1 moL/L NaOH, 0.1 moL/L HC1 was respectively added to the prepared sample, and magnetically stirred for 30, 60, 100, 120 min at room temperature. After it was separated for 10 min at 6,000 rpm by centrifugation, the upper supernatant was taken and poured into a cell and measured with a spectrophotometer to measure its absorbance. The concentration of RB in the upper supernatant was calculated. The desorption ratio was calculated.

2.3.6. Kinetic experiments of adsorption

The kinetic properties of the adsorption of RB by post potassium permanganate-modified peanut shell were studied in the experiment. 10 mL RB solution of 10, 20, 24, and 30 μg/mL was taken and added to 100 mL conical flask. 10 mL pH = 4.0 tri-acid (H_3PO_4-HAc-H_3BO_3)-NaOH buffer solution was used to adjust the acidity of solution. 0.2 g $KMnO_4$ modified peanut shell was added, respectively. After the mixture was stirred for some time at room temperature by magnetic force, respectively, the resulting sample was added into a centrifugal tube. It was separated for 10 min at 6,000 rpm by centrifugation. The centrifugal tube was taken out and the upper supernatant was retained, the concentration of RB in the supernatant was determined according to the determination method for above-mentioned RB working curve, and the adsorption ratio and capacity were calculated, so as to study the adsorption mechanism. This analysis was performed using simplified quasi-first-order and quasi-second-order dynamical models.

2.3.7. Adsorption isothermal experiment

The adsorption isothermal properties of RB by post potassium permanganate-modified peanut shell were studied in the experiment. 10 mL RB solution of 5, 10, 20, and 30 μg/mL was taken and added to 100 mL conical flask. 10 mL pH = 4.0 tri-acid (H_3PO_4-HAc-H_3BO_3)-NaOH buffer solution was used to adjust the acidity of solution. 0.2 g $KMnO_4$ modified peanut shell was added, respectively. For each concentration sample, the mixture was stirred for certain time at the temperature 298.15, 308.15, 318.15, and 328.15 K. The resulting mixed solution was poured into a centrifuge tube. It was separated for 10 min at 6,000 rpm by centrifugation. The centrifugal tube was taken out and the upper supernatant was retained, the concentration of RB in the supernatant was determined according to the determination method for above-mentioned RB working curve, and the adsorption isotherm was prepared.

2.3.8. Adsorption thermodynamic experiment

The thermodynamic properties of the adsorption of RB by post potassium permanganate-modified peanut shell were studied in the experiment. Four portions of 10 mL RB solution of 10 μg/mL were taken and added to 100 mL conical flask. 10 mL pH = 4.0 tri-acid (H_3PO_4-HAc-H_3BO_3)-NaOH buffer solution was used to adjust the acidity of solution. Four portions of 0.2 g $KMnO_4$ modified peanut shell were added, respectively, to the above-mentioned RB. The mixture was stirred for certain time at the temperature 298.15, 308.15, 318.15, and 328.15 K to reach equilibrium. The resulting mixed solution was poured into a centrifuge tube. It was separated for 10 min at 6,000 rpm by centrifugation. The centrifugal tube was taken out and the upper supernatant was retained, the concentration of RB in the supernatant was determined according to the determination method for above-mentioned RB working curve, and adsorption thermodynamic parameters were obtained through relevant calculation.

3. Results and discussion

3.1. Working curve for determination of RB

The absorbance of the RB solution of different concentrations was measured by a 722-type spectrophotometer. The results showed that the RB solution complied with the Lamber–Beer's law at a concentration of 0–10 μg/mL.

The calculated linear regression equation is:

$$A = 0.1039C + 0.0013 \quad (3)$$

where C is the concentration (μg/mL) of RB solution and A is absorbance. R^2 = 0.9997, and the R is a linear regression coefficient.

3.2. Modification of the peanut shell

The decolored peanut shell was modified by hydrochloric acid, phosphoric acid, citric acid, sodium hydroxide, zinc chloride and potassium permanganate respectively. The experimental results showed that the adsorption capacity of the peanut shell has been improved, among which the most obvious improvement is the potassium permanganate modified peanut shell. Potassium permanganate was used to modify the decolored peanut shell in this study. The modified peanut shell adsorption ratio was 99.02% for RB, the adsorption rate was increased by 11.21% compared with unmodified peanut shells.

3.3. Optimization of adsorption condition

3.3.1. Impact of pH

The isoelectric point of peanut shell is 4.2–4.7 [3,6]. When pH is at the isoelectric point, its surface electric charges are zero. It is positively charged at pH less than its isoelectric point. It presents negative charges at pH greater than its isoelectric point. The effect of different pH on the adsorption of RB onto peanut shell was studied. Experimental results (Fig. 1) illustrated that the adsorption of RB is dependent on the pH value of solution. This is due to the solution pH can affect the morphological structure of hydroxyl of the peanut shell surface and the ionization of RB. From the experimental results shown in Fig. 1, the adsorption ratio of waste peanut shell and modified potassium permanganate to RB increased with pH increases. When pH gradually increased, neutralizing H^+ can reduce the competition action of H^+, which facilitates the adsorption of peanut shell to RB. When pH is equal 4.0, the adsorption ratio is maximum. When the pH is greater than 4.0, the adsorption rate begins to decrease gradually. It can be known according to the figure that the potassium permanganate modified peanut shell's adsorption ratio to RB is higher than the unmodified

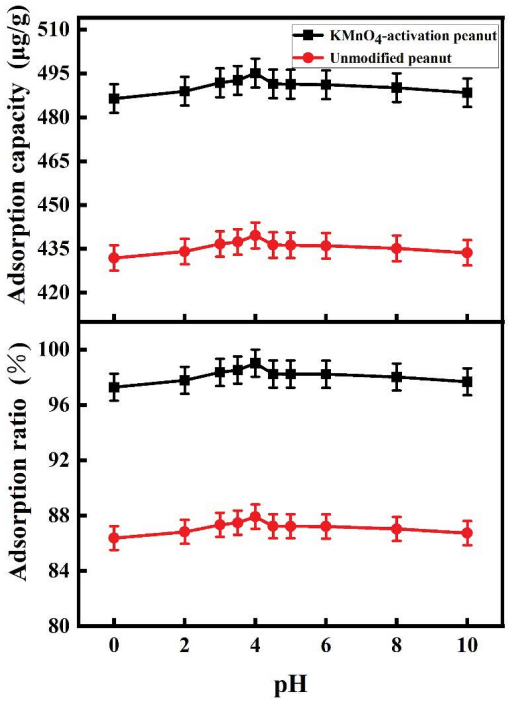

Fig. 1. Effect of pH on the adsorption of RB (adsorbent dosage 10 g/L, temperature condition 25°C ± 1°C, RB concentration = 5 μg/mL, contact time for unmodified and modified adsorbent 110, 100 min).

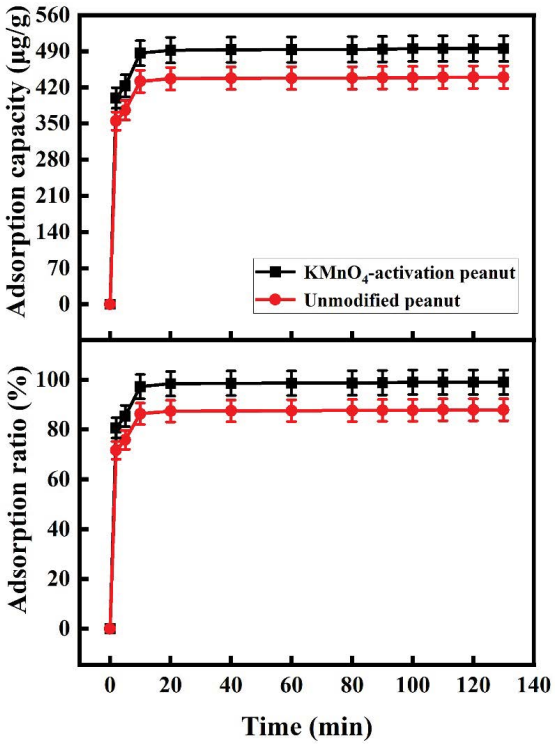

Fig. 2. Effect of contact time on the adsorption of RB (adsorbent dosage = 10 g/L, temperature condition 25°C ± 1°C, pH = 4.0, RB concentration = 5 μg/mL).

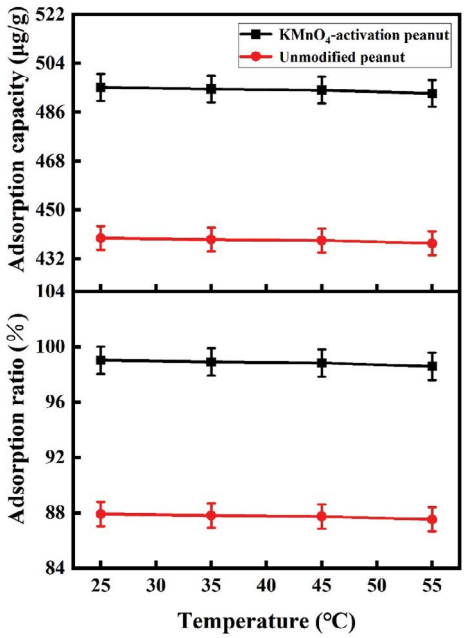

Fig. 3. Effect of temperature on the adsorption of RB (adsorbent dosage = 10 g/L, 25°C ± 1°C, pH = 4.0, RB concentration = 5 μg/mL, contact time for unmodified and modified adsorbent 110, 100 min).

peanut shell's one. When the pH value is between 3 ~ 5, the adsorption amount is high. The adsorption amount is low when the pH values are higher or lower. The possible reason may have two: The first is that under over-acid or over-alkali conditions, RB molecules react with acid or alkali, resulting in the reduce of RB molecule. The second is that under low pH condition the group in the peanut shell preferentially binds to H^+ from solution to form a positive electric active center, and H^+ further complexes with the lone-pair electrons on O atoms, hindering the positive charged RB cation and its combination, so the adsorption amount of RB molecule decreases.

3.3.2. Impact of contact time

The effect of contact time on peanut shell adsorption is shown in Fig. 2. The adsorption capacity of potassium permanganate modified peanut shell for RB continuously increased within 0–100 min. After the contact time was 100 min, the adsorption capacity remained unchanged, which shows that the adsorption system reached the final equilibrium period at 100 min. The unmodified peanut shell adsorption system reached equilibrium at 110 min. In the figure, we can find that for the potassium permanganate modified peanut shell the adsorption capacity gradually increased within 0–100 min, with the extended contact time with RB. The adsorption capacity did not change basically, increasing contact time more than 100 min. For the unmodified peanut shell, increasing contact time extension with RB within 0–110 min, the adsorption capacity was gradually increased. After increasing the contact time over 110 min, the adsorption efficiency remained unchanged and the adsorption reached equilibrium. For its reasons, because the peanut shell contains a large number of available sites at the contact of the RB, the repulsion force between the adsorbate on the peanut shell surface and the solute molecules in the water phase gradually increases with increase in the contact time, and the remaining adsorbable sites decrease, making the remaining adsorption sites on the peanut shell difficult to be used by the RB.

3.3.3. Effects of temperature

It is seen from Fig. 3 that the relationship between temperature and the adsorption quantity or adsorption ratio of RB. The adsorption ratio and adsorption amount of RB onto peanut shell slowly decreased with the increase of temperature and this has two possible reasons. The first is because when the temperature rises, the movement of RB in the solution is more active, and the RB, existing in the form of peanut shell aperture, thus spreads again, and the adsorption capacity and adsorption ratio of RB are reduced. The second is owing to that heating causes the swelling effect of the fibers inside the peanut shell. The adsorption efficiency decreases with the increase in temperature. The adsorption process is an exothermal process.

3.3.4. Effect of adsorbent dosage

From Fig. 4, it can be seen that the results of the effect of adsorbent dosage amount on the effect of RB adsorption

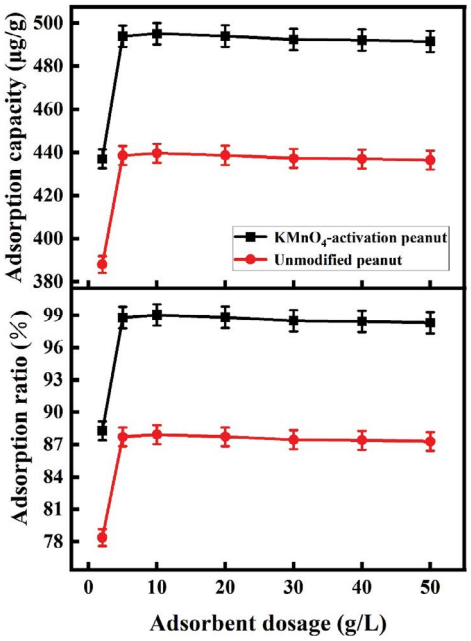

Fig. 4. Effect of sorbent dosage on the adsorption of RB (adsorbent dosage 10 g/L, 25°C ± 1°C, pH = 4.0, RB concentration = 5 μg/mL, contact time for unmodified and modified adsorbent 110, 100 min).

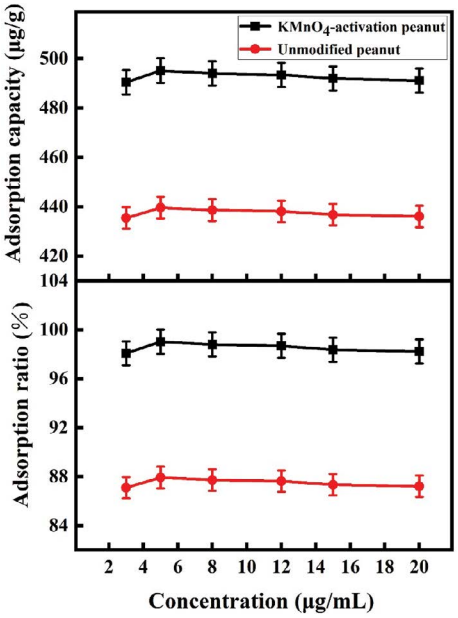

Fig. 5. Effect of initial dye concentration on RB adsorption (adsorbent dosage 10 g/L, 25°C ± 1°C, pH = 4.0, temperature 100°C, contact time for unmodified and modified adsorbent 110, 100 min).

onto peanut shell are seen. When the adsorbent dosage is less than 10 g/L, the adsorption ratio and adsorption capacity of potassium permanganate modified peanut shell constantly increase with the increase of adsorbent dosage. When the dosage of adsorbent is 10 g/L, the adsorption effect is the best. After more than 10 g/L, the adsorption effect is gradually reduced. For unmodified peanut shells, the adsorption law is the same as that of modified adsorption system.

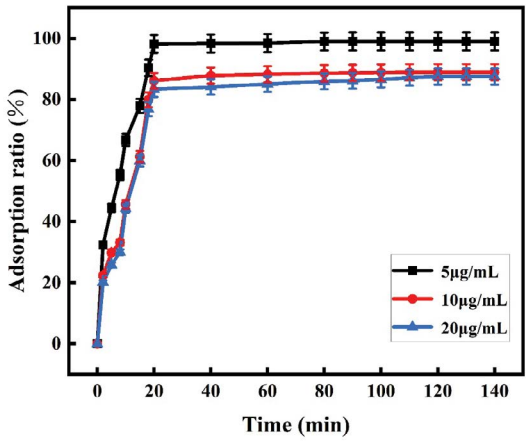

Fig. 6. Relationship between the concentration of different initial dye and contact time (waste peanut adsorbent dosage = 10 g/L, temperature condition 25°C ± 1°C, pH = 4.0).

3.3.5. Effect of initial dye concentration and contact time on adsorption of RB

From Fig. 5, the effect of the initial concentration of RB on its adsorption effect can be seen. When the adsorbent dosage is less than 5 μg/mL, the adsorption ratio and adsorption capacity increase as the initial concentration of RB increases. The adsorption is the best at 5 μg/mL. After that, the adsorption effect gradually decreases. The adsorption laws of unmodified peanut shell and modified peanut shell adsorption system are the same. Fig. 6 shows the relationship between the different initial concentrations of the dye and the contact time, which shows that the adsorption equilibrium time extends as the adsorption concentration increases.

3.3.6. Effect of ionic strength on adsorption of RB

Since salinity ions often exist in organic or dyeing wastewater, the effect of presnce of commonly seen salinity ion Na^+ and Ca^{2+} in solution on the adsorption of RB were studied in the experiment. At the initial concentration 5 μg/mL of RB, the adsorption was affected by the presence of both ions, reducing the adsorption ratio of RB. The effect degree of Ca^{2+} is stronger than Na^+. The effect results of different salinity ion on adsorption are different, and high-valent state and high concentration ion have an inhibitory effect on adsorption. Change of the adsorption rate of RB is within 10% for 2 salinity ions in the range of experimental concentration, so base on this we can know that the degree of RB adsorbed by peanut shell is still very high when the salinity is not very high.

3.4. Desorption results

The results of RB desorption experiment (Fig. 7) show that the desorption effect is good using NaOH compared

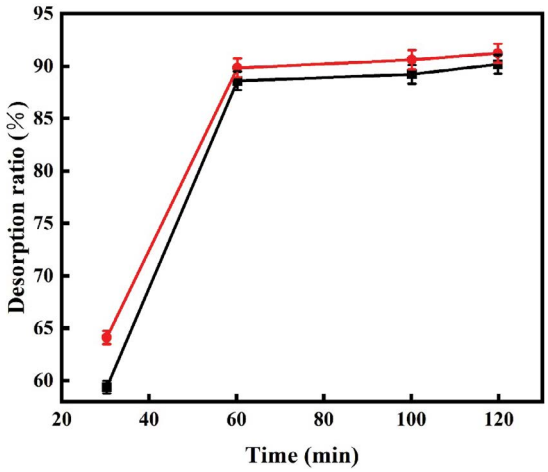

Fig. 7. Desorption of composites by NaOH (-■-potassium permanganate modified peanut shell, -●-unmodified peanut shell, desorption agent is 0.1 mol/L NaOH).

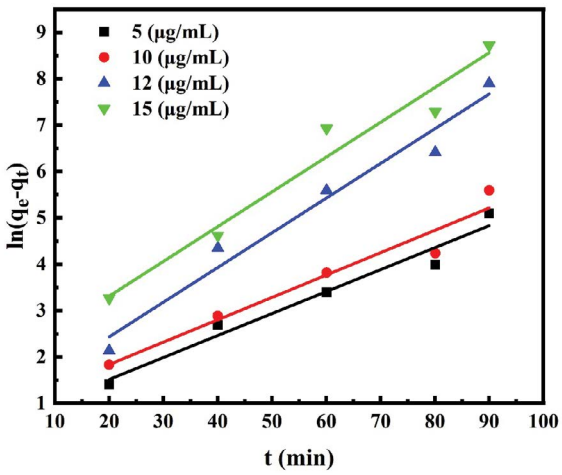

Fig. 8. Pseudo-first-order dynamics (adsorbent dosage: 10 g/L, 25°C ± 1°C, pH = 4.0).

with HCl and NaOH. At 2 h, the corresponding maximum desorption ratio was 90.3% using the NaOH, while the maximum desorption ratio was 55.3% using hydrochloric acid.

3.5. Property of adsorption system

The experiment studied the kinetic properties, isothermal properties and thermodynamic properties of RB by potassium permanganate modified peanut shell.

3.5.1. Adsorption kinetics

Quasi-first-order kinetic model [30–33]:

$$\log\left(q_e - q_t\right) = \log q_e - k_1 t \tag{4}$$

where q_e represents the adsorption amount (μg/g) of RB when realizing adsorption equilibrium, while q_t represents the adsorption amount (μg/g) possessed by RB at t min, k_1 (min^{-1}) represents a quasi-first-order kinetic rate constant, and t is the adsorption contact time (min).

Quasi-second-order kinetic model [34–37]:

$$\frac{t}{q_t} = \frac{1}{k_2 q_e^2} + \frac{t}{q_e} \tag{5}$$

where t is the adsorption contact time (min), k_2 (g/mg·min) is a quasi-second-order kinetic rate constant, q_t represents the adsorption amount (μg/g) of RB at the t min, while q_e represents the adsorption amount (μg/g) of RB when adsorption equilibrium is realized.

The adsorption kinetic experiment is composed of contact time experiment of RB solutions with four different initial concentrations of 5, 10, 12 and 15 μg/mL. The experimental results are linearly fitted with the quasi-first-order kinetic equation and the quasi-second-order kinetic equation. As you can see from Fig. 8, the deviation of fitting the data with the quasi-first-order kinetic equation is relatively large. The experimental results are linearly fitted

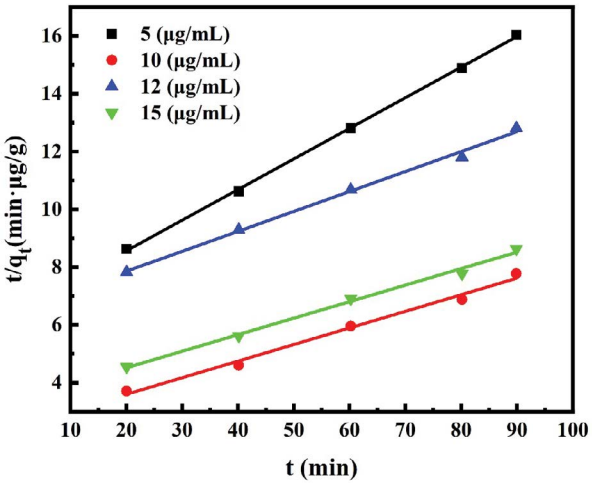

Fig. 9. Pseudo-second-order dynamics (adsorbent dosage: 10 g/L, 25°C ± 1°C, pH = 4.0).

with the quasi-second-order kinetic equation (Fig. 9), and it is seen that the correlation coefficients R_2^2 of the fitted linear equations are all above 0.99. Table 2 gives the quasi-first-order and quasi-second-order kinetic equation data, and the equilibrium adsorption amount and measurement values of each concentration are not very different for the quasi-second-order system, so the adsorption system is more in line with the quasi-second-order kinetic equation.

3.5.2. Isotherm of adsorption

This paper carried out analysis using a linear adsorption isothermal model, including the Langmuir and Freundlich thermodynamic adsorption models.

Langmuir adsorption isothermal formula [38–42]:

$$\frac{C_e}{q_e} = \frac{1}{Q_0 b} + \left(\frac{1}{Q_0}\right) C_e \tag{6}$$

Table 2
Kinetic parameters of adsorption of RB by peanut shell

Concentration (μg/mL)	Measured adsorption capacity (mg/g)	Pseudo-first-order adsorption kinetic equation			Pseudo-second-order adsorption kinetic equation		
		k_1 (min^{-1})	q_e (mg/g)	R_1^2	q_e (mg/g)	k_2 (g/mg·min)	R_2^2
5	0.4901 ± 0.002	0.019 ± 0.001	0.5219 ± 0.0011	0.9643	0.4878 ± 0.003	2.849 ± 0.005	0.9991
10	0.9493 ± 0.004	0.091 ± 0.003	0.6427 ± 0.0015	0.9472	0.9501 ± 0.004	3.764 ± 0.003	0.9912
12	1.4990 ± 0.003	0.052 ± 0.001	0.7014 ± 0.0013	0.9681	1.5012 ± 0.002	6.237 ± 0.001	0.9963
15	2.4911 ± 0.001	0.021 ± 0.002	0.7418 ± 0.0012	0.9630	2.4719 ± 0.001	4.623 ± 0.002	0.9944

where C_e (μg/mL) is the concentration of RB in supernatant at equilibrium, q_e (μg/g) is the equilibrium adsorption amount of RB, Q_0 (μg/g) is theoretical maximum monolayer adsorption capacity, b (mL/μg) is Langmuir constant and it is related with adsorption ability and adsorption rate.

Freundlich adsorption isothermal formula [43–45]:

$$\ln q_e = \ln K_F + \frac{1}{n}\ln C_e \tag{7}$$

where C_e (μg/mL) is the concentration of RB in supernatant at equilibrium, q_e (μg/g) is the equilibrium adsorption amount of RB, K_F and n are Freundlich constants where K_F indicates adsorption degree and $1/n$ indicates adsorption strength and generally less than 1.

The adsorption isothermal experiment is composed of temperature tests of four different RB solutions with 5, 10, 12, and 15 μg/mL. Fig. 10 shows the linear fitting of experimental results using Langmuir adsorption isotherm. Fig. 11 shows the linear fitting of experimental results using Freundlich adsorption, and the Langmuir and Freundlich adsorption isothermal data are shown in Table 3. Compared with Figs. 10 and 11, it can be concluded that after the experimental data is fitted the correlation coefficient of Freundlich adsorption isotherm is greater than 0.99, so the adsorption process can be better expressed by Freundlich adsorption isotherm.

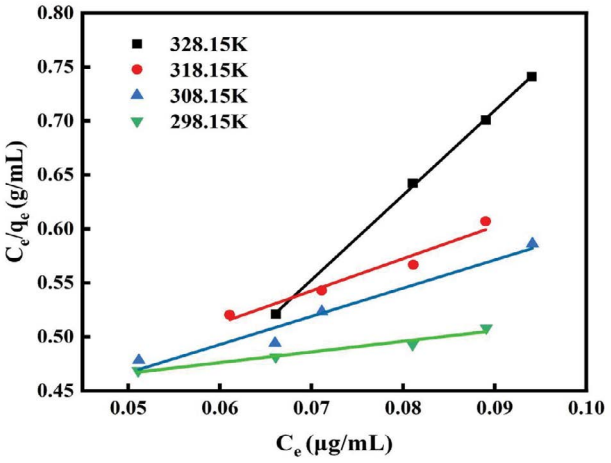

Fig. 10. Langmuir adsorption isotherm (adsorbent dosage 10 g/L, pH = 4.0, adsorption time 100 min).

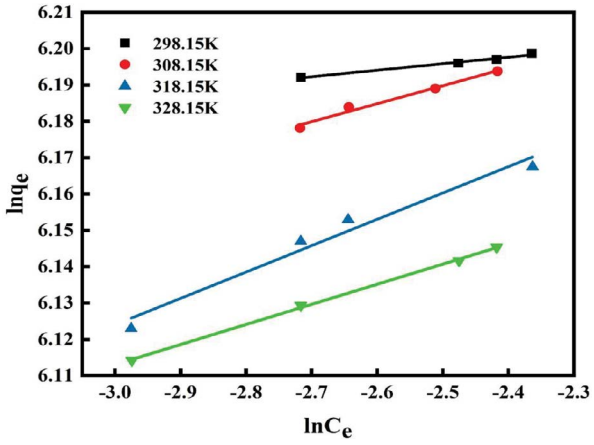

Fig. 11. Freundlich adsorption isotherm (adsorbent dosage 10 g/L, pH = 4.0, adsorption time 100 min).

3.5.3. Thermodynamics of adsorption

The $\Delta G°$, $\Delta H°$, $\Delta S°$ during adsorption is derived from the following formula [46,47]:

$$K_d = \frac{q_e}{C_e} \tag{8}$$

$$\ln K_d = \frac{\Delta S}{R} - \frac{\Delta H}{RT} \tag{9}$$

$$\Delta G° = \Delta H° - T\Delta S° \tag{10}$$

where K_d is the temperature-dependent adsorption equilibrium constant, q_e (μg/g) is the equilibrium adsorption amount of RB, C_e (μg/mL) is the concentration of RB in supernatant at equilibrium, $\Delta S°$ is the adsorption entropy variation value [J/(mol·K)], R is the ideal gas constant (8.314 J/mol·K), $\Delta H°$ is the enthalpy variation value (kJ/mol) of the adsorption process, T is absolute temperature (K), $\Delta G°$ is the free energy variation value of the adsorption process (kJ/mol).

The results of the adsorption thermodynamic parameters studied and obtained in this article are listed in Table 4. It can be seen that all $\Delta G°$ is less than 0, so the reaction taking place in the adsorption process is spontaneous reaction. It is generally thought that the reaction taking place during 0 to –20 kJ/mol of $\Delta G°$ is physical adsorption reaction, the reaction taking place during –20 to –80 kJ/mol of $\Delta G°$ is physical chemical adsorption, the reaction taking place during –80 to

Table 3
Relevant parameters of adsorption isotherm

T (K)	Langmuir adsorption isotherm			Freundlich adsorption isotherm		
	Q_0 (mg/g)	b	R	K_F (L/g)$^{(1-1/n)}$	$1/n$	R
298.15	0.6601	62.05	0.9798	517.3	0.0187	0.9991
308.15	0.3812	36.26	0.9698	541.2	0.0420	0.9998
318.15	0.3761	46.76	0.9584	569.2	0.0734	0.9990
328.15	0.4873	67.66	0.9852	555.3	0.0704	0.9993

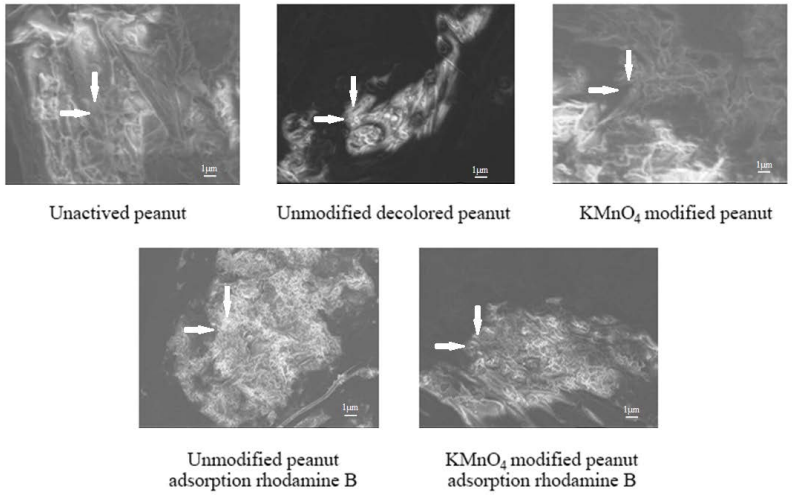

Fig. 12. Scanning electric microscopic diagram.

Table 4
Adsorption thermodynamic parameters

T (K)	$\Delta G°$ (kJ/mol)	$\Delta H°$ (kJ/mol)	$\Delta S°$ (J/mol·K)
298.15	–30.68	–62.48	–1.379
308.15	–32.57		
318.15	–35.68		
328.15	–36.72		

–400 kJ/mol of $\Delta G°$ is chemical adsorption [48]. Therefore, the adsorption of potassium permanganate modified peanut shell to RB should be physical chemical adsorption. From Table 4, it can be known that the adsorption enthalpy change $\Delta H°$ is negative, indicating that the adsorption process is an exothermic reaction, which also confirms that the adsorption effect of RB decreases with the increase of temperature. The Gibbs free energy changes at 3 temperatures are all less than zero, and the higher the temperature, the smaller the $\Delta G°$. This reveals that the adsorption process of RB by adsorbent is spontaneous and the higher the temperature, the greater the spontaneous degree. The size of its value also reflects the size of the driving force of the adsorption process. The greater the absolute value of $\Delta G°$, the greater the adsorption driving force. The experimental data show that when the temperature is higher, the adsorption driving force is higher. $\Delta S°$ is negative value, which shows that the degree of freedom of the adsorbate also increases and that the adsorption is an entropy driven process.

3.6. Characterization of material

Scanning electric microscopic images can reflect the characteristics of the surface of the sample (Fig. 12). The aperture structure of the peanut shell is the main site combining the peanut shell and RB. After adsorption, a large number of RB was observed in the electric microscopic images, indicating that the adsorption effect is very good. According to infrared spectra (Fig. 13), we can compare untreated peanut shell, decolored and unmodified peanut shell, potassium permanganate modified peanut shell, unmodified peanut shell adsorption RB, we may reach the following conclusion that after the potassium permanganate modified peanut shell and adsorption RB, the original structure of peanut shell was still retained. Powder X-ray diffraction analysis results show that the characteristic diffraction peak is shown as Fig. 14. Compared with the untreated peanut shell, boiled but unmodified peanut shell, we can see that the main characteristic peak disappeared after boiling, indicating that its structure was destroyed. Compared with the boiled but unmodified peanut shell, potassium permanganate modified peanut shell, unmodified peanut shell adsorption RB, it can be seen that the characteristic peak strength has decreased but the position is unchanged, which shows that the peanut shell structure has not been changed and the order degree is reduced.

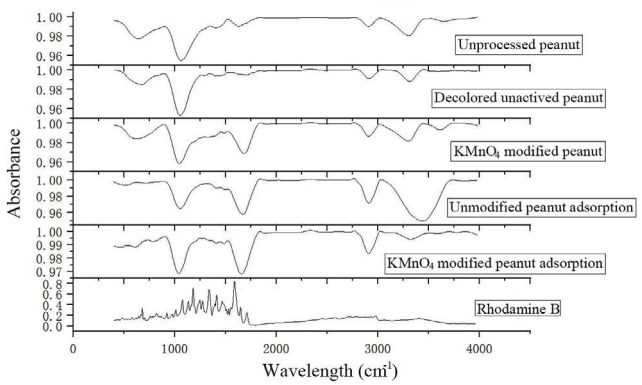

Fig. 13. Infrared spectra.

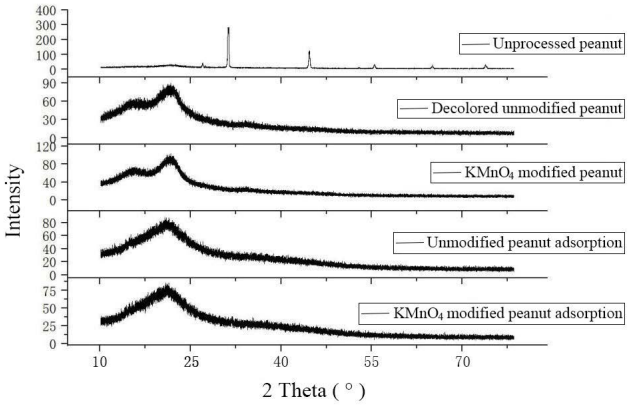

Fig. 14. X-ray diffraction diagram.

Compared with acid and organic modified halloysite [49] and amorphous titanium dioxide powder [50] RB adsorbents, this system has higher adsorption capacity of RB and potential application value.

3.7. Study of practicability of method

In order to verify the practicability of the method, we adsorbed the wastewater containing Rhodamine B discharged from a factory (a factory in Changchun City, China) according to the experimental method, and achieved good results. The original sample contained 10 μg/mL Rhodamine B, and after the adsorption of Rhodamine B according to this method, its content decreased to 3.2 ng/mL. It can be seen that this method has a good adsorption capacity of Rhodamine B and has a good potential application value of adsorption Rhodamine B. The price of reagents used in this study are very cheap. Carrying out one adsorption experiment consumes about 0.37 Chinese yuan (0.05 $).

4. Conclusions

With a goal of peanut shell as a new biological adsorbent, modification by potassium permanganate, the optimum adsorption conditions of RB by these two materials, thermodynamics, isothermal properties and thermodynamic properties were studied in this paper. The conclusions found are as follows:

- Under the optimized adsorption conditions, the adsorption rate of the modified peanut shell was increased by 11.21%, its adsorption capacity is 495.1 μg/g, and the adsorption rate is 99.02%.
- The thermodynamic parameter $\Delta G° < 0$, adsorption enthalpy change $\Delta H° = -62.481$ kJ/mol, and adsorption change $\Delta S° = -1.379$ J/(mol·K), adsorption process is a spontaneous exothermal entropy reduction process.
- RB adsorbed by peanut shell is in accord with quasi-second-order dynamics. The adsorption of RB by the modified peanut shell conforms to the Freundlich isothermal adsorption equation.

Declarations

Supplementary information

Not applicable.

Funding

The author thanks the financial support "Research on the Adsorption of Water and Soil Pollutants Heavy Metals and Harmful Dyes by Waste Tea and Peanut Shell" by the Natural Science Foundation of Jilin Provincial Science and Technology Department from the Science and Technology Development Program of Jilin Province, China (20220101096JC/611220683029/KYC-JC-XM-2022-111).

Availability of data and materials

The datasets used or analyzed during the current study are available from the corresponding author on reasonable request.

Ethics approval and consent to participate

Not applicable.

Consent for publication

The author has read this manuscript and consent for publication in Desalination and Water Treatment.

Competing interests

The author declares no competing interests.

References

[1] Z. Yang, Y.G. Wang, Y.J. Jing, Q.W. Wei, F.F. Leng, H. Ma, Y.L. Wang, J.X. Chen, Preparation and modification of peanut shells and their application for heavy metals adsorption, Bulg. Chem. Commun., 48 (2016) 535–542.
[2] H. Ali, Biodegradation of synthetic dyes—a review, Water Air Soil Pollut., 213 (2010) 251–273.
[3] X.J. Li, H.Q. Xue, L. Huang, A.J. Qian, Study on adsorption of Pb^{2+} in water by NaOH modified peanut shell, Coal Chem. Ind., 38 (2015) 51–54.

[4] R. Jain, M. Mathur, S. Sikarwar, A. Mittal, Removal of the hazardous dye Rhodamine B through photocatalytic and adsorption treatments, J. Environ. Manage., 85 (2007) 956–964.
[5] P. Saharan, V. Kumar, J. Mittal, V. Sharma, A.K. Sharma, Efficient ultrasonic assisted adsorption of organic pollutants employing bimetallic-carbon nanocomposites, Sep. Sci. Technol., 56 (2021) 2895–2908.
[6] J. Lei, X.Y. Yi, C. Yang, G.N. Lu, Z. Dang, Adsorption mechanism of and Cd^{2+} and Pb^{2+} modified peanut shells, Chin. J. Environ. Eng., 8 (2014) 1775–1783.
[7] H. Lv, Preparation and characterization of quaternary ammonium peanut shell sorbent, Guangzhou Chem. Eng., 42 (2014) 63–65.
[8] T.O. Ajiboye, O.A. Oyewo, D.C. Onwudiwe, Adsorption and photocatalytic removal of Rhodamine B from wastewater using carbon-based materials, FlatChem, 29 (2021) 100277, doi: 10.1016/j.flatc.2021.100277.
[9] J. Mittal, Permissible synthetic food dyes in India, Resonance – J. Sci. Edu., 25 (2020) 567–577.
[10] A. Mittal, R. Jain, J. Mittal, S. Varshney, S. Sikarwar, Removal of yellow ME 7 GL from industrial effluent using electrochemical and adsorption techniques, Int. Environ. Pollut., 43 (2010) 308–323.
[11] Q.-S. Wang, Q.-Z. Zhai, Study on the assembly of hemoglobin by nano mesoporous SBA-15 and catalytic activity, J. Sol-Gel Sci. Technol., 84 (2017) 70–86.
[12] K. Kadirvelu, M. Kavipriya, C. Karthika, M. Radhika, N. Vennilamani, S. Pattabhi, Utilization of various agricultural wastes for activated carbon preparation and application for the removal of dyes and metal ions from aqueous solutions, Bioresour. Technol., 87 (2003) 129–132.
[13] T. Robinson, G. McMullan, R. Marchant, P. Nigam, Remediation of dyes in textile effluent: a critical review on current treatment technologies with a proposed alternative, Bioresour. Technol., 77 (2001) 247–255.
[14] H.F. Lv, J.P. Zhai, Effect of acid formaldehyde modification on the adsorption of heavy metal ions by peanut shell, Environ. Pollut. Prevent., 29 (2007) 837–840.
[15] A.M. Azzam, S.T. El-Wakeel, B.B. Mostafa, M.F. El-Shahat, Removal of Pb, Cd, Cu and Ni from aqueous solution using nano scale zero valent iron particles, J. Environ. Chem. Eng., 4 (2016) 2196–2206.
[16] Y.R. Li, P. Bai, Y. Yan, W.F. Yan, W. Shi, R.R Xu, Removal of Zn^{2+}, Pb^{2+}, Cd^{2+}, and Cu^{2+} from aqueous solution by synthetic clinoptilolite, Microporous Mesoporous Mater., 273 (2019) 203–211.
[17] S.G. Wang, K.K. Wang, C. Dai, H.Z. Shi, J.L. Li, Adsorption of Pb^{2+} on amino-functionalized core–shell magnetic mesoporous SBA-15 silica composite, Chem. Eng. J., 262 (2015) 897–903.
[18] A. Mariyam, J. Mittal, F. Sakina, R.T. Baker, A.K. Sharma, A. Mittal, Efficient batch and fixed-bed sequestration of a basic dye using a novel variant of ordered mesoporous carbon as adsorbent, Arabian J. Chem., 14 (2021) 103186, doi: 10.1016/j.arabjc.2021.103186.
[19] C. Arora, D. Sahu, D. Bharti, V. Tamrakar, S. Soni, S. Sharma, Adsorption of hazardous dye crystal violet from industrial waste using low-cost adsorbent *Chenopodium album*, Desal. Water Treat., 167 (2019) 324–332.
[20] A. Patel, S. Soni, J. Mittal, A. Mittal, C. Arora, Sequestration of crystal violet from aqueous solution using ash of black turmeric rhizome, Desal. Water Treat., 220 (2021) 342–352.
[21] J. Mittal, R. Ahmad, M.O. Ejaz, A. Mariyam, A. Mittal, A novel, eco-friendly bio-nanocomposite (Alg-Cst/Kal) for the adsorptive removal of crystal violet dye from its aqueous solutions, Int. J. Phytorem., 24 (2022) 796–807.
[22] S. Soni, P.K. Bajpai, D. Bharti, J. Mittal, C. Arora, Removal of crystal violet from aqueous solution using iron-based metal organic framework, Desal. Water Treat., 205 (2020) 386–399.
[23] J. Mittal, R. Ahmad, A. Mittal, Kahwa tea (*Camellia sinensis*) carbon — a novel and green low-cost adsorbent for the sequestration of titan yellow dye from its aqueous solutions, Desal. Water Treat., 227 (2021) 404–411.
[24] R. Jain, P. Sharma, S. Sikarwar, J. Mittal, D. Pathak, Adsorption kinetics and thermodynamics of hazardous dye Tropaeoline 000 unto Aeroxide Alu C (Nano alumina): a non-carbon adsorbent, Desal. Water Treat., 52 (2014) 7776–7783.
[25] A. Mariyam, J. Mittal, F. Sakina, R.T. Baker, A.K. Sharma, Adsorption behaviour of Chrysoidine R dye on a metal/halide-free variant of ordered mesoporous carbon, Desal. Water Treat., 223 (2021) 425–433.
[26] S. Soni, N. Rai, P.K. Bajpai, J. Mittal, C. Arora, Enhanced sequestration of an acidic dye on novel bimetallic metal-organic framework, J. Dispersion Sci. Technol., 44 (2023) 1500–1504.
[27] Mu. Naushad, A.A. Ansari, Z.A. ALOthman, J. Mittal, Synthesis and characterization of YVO_4:Eu^{3+} nanoparticles: kinetics and isotherm studies for the removal of Cd^{2+} metal ion, Desal. Water Treat., 57 (2016) 2081–2088.
[28] R. Ahmad, I. Hasan, A. Mittal, Adsorption of Cr(VI) and Cd(II) on chitosan grafted polyaniline-OMMT nanocomposite: isotherms, kinetics and thermodynamics studies, Desal. Water Treat., 58 (2017) 144–153.
[29] J. Mittal, R. Ahmad, A. Mariyam, V.K. Gupta, A. Mittal, Expeditious and enhanced sequestration of heavy metal ions from aqueous environment by papaya peel carbon: a green and low-cost adsorbent, Desal. Water Treat., 210 (2021) 365–376.
[30] S. Lagergren, Zur theorie der sogenannten adsorption geloester stoffe (About theory of so-called adsorption of soluble substances), Kungliga Svenska Vetenskapsakad, Handl, 24 (1898) 1–39.
[31] N. Naushad, Surfactant assisted nano-composite cation exchanger: development, characterization and applications for the removal of toxic Pb^{2+} from aqueous medium, Chem. Eng. J., 235 (2014) 100–108.
[32] K.T. Wong, N.C. Eu, S. Ibrahim, H. Kim, Y. Yoon, M. Jang, Recyclable magnetite-loaded palm shell-waste based activated carbon for the effective removal of methylene blue from aqueous solution, J. Cleaner Prod., 115 (2016) 337–342.
[33] E. Haque, V. Lo, A.I. Minett, A.T. Harris, T.L. Church, Dichotomous adsorption behaviour of dyes on an amino-functionalised metal–organic framework, amino-MIL-101(Al), J. Mater. Chem. A, 2 (2014) 193–203.
[34] Y.S. Ho, G. McKay, Pseudo-second-order model for sorption processes, Process Biochem., 34 (1999) 451–465.
[35] C. Li, Z.H. Xiong, J.M. Zhang, C.S. Wu, the strengthening role of the amino group in metal–organic framework MIL-53 (Al) for methylene blue and malachite green dye adsorption, J. Chem. Eng. Data, 60 (2015) 3414–3422.
[36] A. Çelekli, B. Tanrıverdi, H. Bozkurt, Predictive modeling of removal of Lanaset Red G on *Chara contraria*; kinetic, equilibrium, and thermodynamic studies, Chem. Eng. J., 169 (2011) 166–172.
[37] E.I. El-Shafey, S.N.F. Ali, S. Al-Busafi, H.A.J. Al-Lawati, Preparation and characterization of surface functionalized activated carbons from date palm leaflets and application for methylene blue removal, J. Environ. Chem. Eng., 4 (2016) 2713–2724.
[38] I. Langmuir, The adsorption of gases on plane surfaces of glass, mica and platinum, J. Am. Chem. Soc., 40 (1918) 136–403.
[39] E. Altıntıg, H. Altundag, M. Tuzen, A. Sarı, Effective removal of methylene blue from aqueous solutions using magnetic loaded activated carbon as novel adsorbent, Chem. Eng. Res. Des., 122 (2017) 151–163.
[40] L. Liu, S. Fan, Y. Li, Removal behavior of methylene blue from aqueous solution by tea waste: kinetics, isotherms and mechanism, Int. J. Environ. Res. Public Health, 15 (2018) 1321–1327.
[41] X. Chen, Modeling of experimental adsorption isotherm data, Information, 6 (2015) 14–22.
[42] E. Daneshvar, A. Vazirzadeh, A. Niazi, M. Kousha, Mu. Naushad, A. Bhatnagar, Desorption of methylene blue dye from brown macroalga: effects of operating parameters, isotherm study and kinetic modeling, J. Cleaner Prod., 152 (2017) 443–453.
[43] H.M.F. Freundlich, Over the adsorption in solution, J. Phys. Chem., 57 (1906) 385–470.

[44] A. Asmat, B. Muhammad, K. Romana, F. Robina, S. Maria, Ultrasound-assisted adsorption of phenol from aqueous solution by using spent black tea leaves, Environ. Sci. Pollut. Res., 25 (2018) 22920–22930.
[45] W.J. Lei, X. Huo, X.Y. Zhou, Adsorption characteristics and its parameters estimation of 3,5,6-trichloro-2-pyridinol in purple soil, Trans. Chin. Soc. Agric. Mach., 48 (2017) 267–274.
[46] D. Bendaho, T.A. Driss, D. Bassou, Adsorption of acid dye onto activated Algerian clay, Bull. Chem. Soc. Ethiop., 31 (2017) 51–57.
[47] D.C. Santos, M.A. Adebayo, E.C. Lima, Application of carbon composite adsorbents prepared from coffee waste and clay for the removal of reactive dyes from aqueous solutions, J. Braz. Chem. Soc., 26 (2015) 924–938.
[48] Ö. Gerçel, A. Özcan, A. Safa Özcan, H. Ferdi Gerçel, Preparation of activated carbon from a renewable bio-plant of *Euphorbia rigida* by H_2SO_4 activation and its adsorption behavior in aqueous solutions, Appl. Surf. Sci., 253 (2007) 4843–4852.
[49] E. Wierzbicka, K Kusmierek, A. Świątkowski, I. Legocka, Efficient Rhodamine B dye removal from water by acid- and organo-modified halloysites, Minerals, 12 (2022) 350, doi: 10.3390/min12030350.
[50] Z.F. Wang, C.Y. Xiao, S. Yamada, K. Yoshinaga, X.R. Bu, M. Zhang, Concentration-driven phase control for low temperature synthesis of phase-pure anatase and rutile titanium oxide, J. Colloid Interface Sci., 448 (2015) 280–286.